Novel transparent nanocomposite films based on chitosan and bacterial cellulose

Susana C. M. Fernandes,[a,b] Lúcia Oliveira,[a] Carmen S. R. Freire,*[a] Armando J. D. Silvestre,[a] Carlos Pascoal Neto,[a] Alessandro Gandini[a] and Jacques Desbriéres[b]

New nanocomposite films based on different chitosan matrices (two chitosans with different DPs and one water soluble derivative) and bacterial cellulose were prepared by a fully green procedure by casting a water based suspension of chitosan and bacterial cellulose nanofibrils. The films were characterized by several techniques, namely SEM, AFM, X-ray diffraction, TGA, tensile assays and visible spectroscopy. They were highly transparent, flexible and displayed better mechanical properties than the corresponding unfilled chitosan films. These new renewable nanocomposite materials also presented reasonable thermal stability and low O_2 permeability.

Introduction

Over the past few years, a renewed and increasing interest on the exploitation of biomass resources for the development of new materials has been observed. This global tendency appears as a natural response for the predictable scarcity of fossil resources and also to the environmental problems associated with their continuous use during the last century. Polysaccharides, in particular cellulose, but also chitin and its derivative chitosan, as well as starch, are of increasing interest as new functional polymeric renewable materials because of their abundance and specific properties.[1]

Chitosan exhibits unique physicochemical properties like biocompatibility, antimicrobial activity, biodegradability and excellent film-forming ability, which have attracted scientific and industrial interest in fields such as biotechnology, pharmaceutics, biomedicine, packaging, wastewater treatment, cosmetics, and food science, among others[2] and a large number of derivatives have been described.[3] However, despite the numerous advantages and unique properties, its films are often brittle, which limits their applications. One way to improve the mechanical properties (and other functionalities) of chitosan films, is to prepare blends with other polymers. In the past few years, a considerable number of studies dealing with the blending of chitosan with various synthetic and natural polymers, such as poly(vinyl alcohol),[4,5] poly(N-vinyl pyrrolidone),[6] poly(ethylene oxide),[7] starch,[5] collagen,[8] water-soluble tertiary polyamides,[9] cellulose[10–13] and its derivatives,[4,5] has been published.

Chitosan–cellulose blends are of particular interest[10–13] because of the structural similarity of these two biopolymers,

resulting in materials that combine the physicochemical properties of chitosan with the excellent mechanical properties of natural fibers. Several authors have studied the structure of these blends, obtained in solution[10,11,13] or in the solid phase,[14] and found evidence of interactions, mainly on the interfacial region between chitosan and cellulose.[15]

More recently, the incorporation of micro and nano-cellulose fibers, obtained by mechanical, enzymatic or chemical treatments, into several polymeric matrices, including chitosan, allowed obtaining materials with superior mechanical properties and transparency.[16–18] The search for new renewable transparent films for electronic devices and also packaging applications is a very recent and promising research field.[19–21]

Bacterial cellulose, produced by *Acetobacter xylinum*, is becoming a promising biopolymer for several applications, including optically transparent nanocomposites,[22–25] due to its unique properties, such as high mechanical strength, high crystallinity and a highly pure nanofibrillar network structure. However, to the best of our knowledge, the preparation and characterization of highly transparent chitosan–bacterial cellulose films has never been reported. The published studies deal only with the preparation of chitosan–bacterial cellulose mixed materials through (i) the modification of the bacterial cellulose biosynthesis conditions, by the addition of polyaminosaccharide modifiers into the culture medium[26,27] and (ii) dipping a dried bacterial cellulose membrane into an acetic acid solution of chitosan.[28] The resulting membranes were characterized and showed valuable features including superior mechanical properties in a wet and a dry state, a high water absorption capacity, a high average surface area, high moisture-keeping properties as well as bacteriostatic and bactericidal activity.[27,28]

In the present paper, we describe the preparation and characterization of new transparent nanocomposite films based on different chitosan matrices and bacterial cellulose nano- and micro-fibrils as reinforcing agents. Two chitosan samples, with distinct molecular weights and thus originating solutions with different viscosities, were used, with the aim of preparing

[a]Department of Chemistry and CICECO, Campus de Santiago, University of Aveiro, 3810-193, Aveiro, Portugal. E-mail: cfreire@ua.pt; Fax: + 351 234 370 084; Tel: + 351234370604
[b]University of Pau and Adour Countries (UPPA), IPREM (UMR CNRS 5254), Helioparc Pau Pyrenées-2, Avenue P. Angot, 64053, Pau Cedex 09, France

nanocomposites with different bacterial cellulose contents. In addition, a water soluble chitosan was also used in order to avoid the use of acetic acid solutions and because these derivatives displayed enhanced antimicrobial properties.[29]

These new materials were obtained through a simple and fully green approach by casting a water-based suspension of chitosan and bacterial cellulose nanofibrils.

Experimental

Materials

Two different chitosans (CH) were used in this work, a relatively low molecular weight sample (LCH), kindly provided by Norwegian Chitosan AS (Norway), and a high molecular weight (HCH) one, purchased from Mahtani Chitosan PVT.Ltd. (India). These commercial samples were purified by dissolution in a 1% (v/v) aqueous CH_3CO_2H solution, filtered and precipitated by neutralizing with NaOH up to a pH of 8.5. The ensuing precipitates were washed with distilled water until a neutral pH and air dried. Their viscosity-average molar mass, obtained at 25 °C from a 0.3 M CH_3CO_2H/0.2 M CH_3CO_2Na solution, using the published Mark–Houwink constants,[30] were 90 000 g/mol for LCH and 350 000 g/mol for HCH. The degrees of deacetylation (DDA), determined by ^1H NMR (in D_2O containing 1% of CD_3COOD) using a DRX-300 Brüker spectrometer, were found to be 90 and 97% for LCH and HCH, respectively.[31]

In order to synthesize a water soluble quaternary ammonium derivative of chitosan (Fig. 1), following the procedure described by Seong et al.,[29] 5.0 g of purified chitosan (HCH) were dissolved in 250 ml of an aqueous solution of 1% acetic acid; glycidyltrimethylammonium chloride (GTMAC-purchased from Fluka, 90% purity), with a GTMAC/HCH molar proportion of 4/1, was added with stirring. This mixture was kept at 65 °C for 24 h under a N_2 atmosphere. The ensuing water soluble chitosan (WSHCH) derivative was precipitated and washed with ethanol (purchased from Sigma–Aldrich, 90% purity). The substitution degree of the amino groups was around 30%, as determined by ^1H NMR spectroscopy following a previously described method.[31]
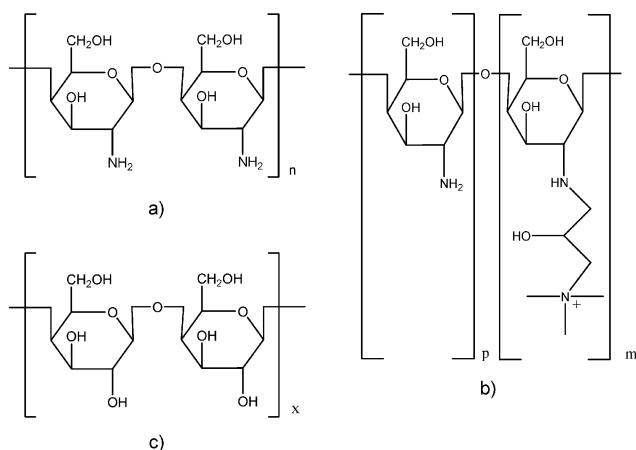
Bacterial cellulose (BC) (tridimensional network of nano- and microfibrils with 10–200 nm width) in the shredded wet form (95% humidity), was supplied by Forschungszentrum für Medizintechnik und Biotechnologie e.V. (Germany).

Chitosan/bacterial cellulose nanocomposite films preparation

For the preparation of the HCH, LCH and WSHCH nanocomposite films, 1.5% solutions were first prepared, by dissolving the corresponding powdered chitosan samples in aqueous acetic acid (1% v/v) or in water (in the case of WSHCH). Different amounts of bacterial cellulose were added to these solutions in order to obtain films with BC contents of 5 and 10% for the HCH and WSHCH films and 5, 10, 30 and 40% for the LCH films, with respect to the dry weight of chitosan (the maximum amount of BC used with each type of chitosan was limited by the final high viscosity of the ensuing mixtures as, above these maximum values, they could not be processed under the reported conditions). Then, BC was dispersed in the solutions and homogenized using an Ultra-Turrax equipment during 45 minutes (20 500 rpm), filtered to remove impurities and degassed to remove entrapped air. Both unfilled CH and nanocomposite films based on chitosan and bacterial cellulose (CHBC films) were then prepared by casting at 30 °C in a ventilated oven for 16 h, using an acrylic plate (10×10 cm^2) as the mould. The identification of all samples studied is summarised in Table 1.

Before characterization, all films were kept in a conditioning cabinet at 50% relative humidity (RH) and 25 °C to ensure the stabilization of their water content.

Films characterization

The CH and CHBC films were characterized using scanning electron microscopy (SEM), atomic force microscopy (AFM), X-ray diffraction (XRD), transmittance (visible light), thermogravimetry (TGA) and tensile tests.

SEM micrographs of the film surfaces were obtained on a HR-FESEM SU-70 Hitachi equipment operating at 1.5 kV and that of BC was taken with a Hitachi S4100 equipment operating in the field emission mode.

AFM measurements were performed on an Innova AFM Veeco Instrument. The images were scanned in a tapping

Fig. 1 Chemical structures of (a) chitosan, (b) its water soluble-derivative and (c) cellulose.

Table 1 Identification of the CH-based films

Sample	CH sample	% of BC[a]
HCH	High molecular weight	—
HCHBC5%	High molecular weight	5
HCHBC10%	High molecular weight	10
LCH	Low molecular weight	—
LCHBC5%	Low molecular weight	5
LCHBC10%	Low molecular weight	10
LCHBC30%	Low molecular weight	30
LCHBC40%	Low molecular weight	40
WSHCH	High molecular weight (water soluble derivative)	—
WSHCHBC5%	High molecular weight (water soluble derivative)	5
WSHCHBC10%	High molecular weight (water soluble derivative)	10

[a] In relation to the oven dry chitosan mass.

mode under ambient conditions using rectangular silicon cantilevers from veeco-probes (MMP-12100-10), resonating at about 110 kHz.

The X-ray diffraction (XRD) measurements were carried out with a Philips X'pert MPD diffractometer using Cu Kα radiation.

The transmittance spectra of the CH films and CHBC films were measured with a UV-vis Spectrophotometer (Perkin-Elmer UV 850) equipped with a 15 cm diameter integrating sphere bearing the holder in the horizontal position. Spectra were recorded at room temperature in steps of 1 nm, in the range 400–700 nm.

TGA assays were carried out with a Shimadzu TGA 50 analyzer equipped with a platinum cell. Samples were heated at a constant rate of 10 °C/min from room temperature to 800 °C under a nitrogen flow of 20 mL/min. The thermal decomposition temperature was taken as the onset of significant (~0.5%) weight loss, after the initial moisture loss.

Tensile tests were performed in room conditions on a TA-Hdi Stable Micro Systems Texture Analyser using a load cell of 5 kg and operating at a deformation rate of 0.5 mm/s. Tensile strength, tensile modulus, and elongation to break were calculated using the Instron Series IX software.

Results and discussion

Morphology

A selection of SEM micrographs of the surface of LCHBC films filled with 5%, 10% and 40% of BC and of WSHCH film filled with 5% of BC is shown in Fig. 2. The characteristic tridimensional fibrillar network of BC was clearly observed on the surface of the films. The SEM micrographs also provided evidence of the good dispersion of the BC fibrils on the matrices, without noticeable aggregates, even for high reinforcement contents.

The surface of the films was also inspected by AFM (Fig. 3). The surface of the unfilled CH films displayed a typical granular morphology (around 100–300 nm),[32] while that of the CHBC nanocomposite films consisted mainly of randomly assembled nanofibrils (10–200 nm) of BC and CH granules.

X-Ray diffraction

The X-ray diffraction patterns of unfilled CH films, BC and CHBC nanocomposite films are shown in Fig. 4 and 5. Both HCH and LCH showed the typical X-ray diffraction pattern of chitosan substrates with strong peaks at around 2θ 12 and 19°.[33] However, the HCH film was much more crystalline than the LCH counterpart (Fig. 4). The chemical modification of HCH with glycidyltrimethylammonium chloride led to an extensive decline of the crystallinity, since the WSHCH film displayed a diffraction pattern typical of a predominantly amorphous material, as previously observed with other water-soluble chitosan derivatives.[34] BC exhibited a diffractogram typical of Cellulose I (native cellulose), with the main peaks at 2θ 14.3, 15.9, 22.6 and 33.7° (Fig. 4).[35]

The X-ray diffractograms of all CHBC nanocomposite films showed typical diffraction peaks of both polysaccharide components (Fig. 5). The incorporation of BC seemed also to
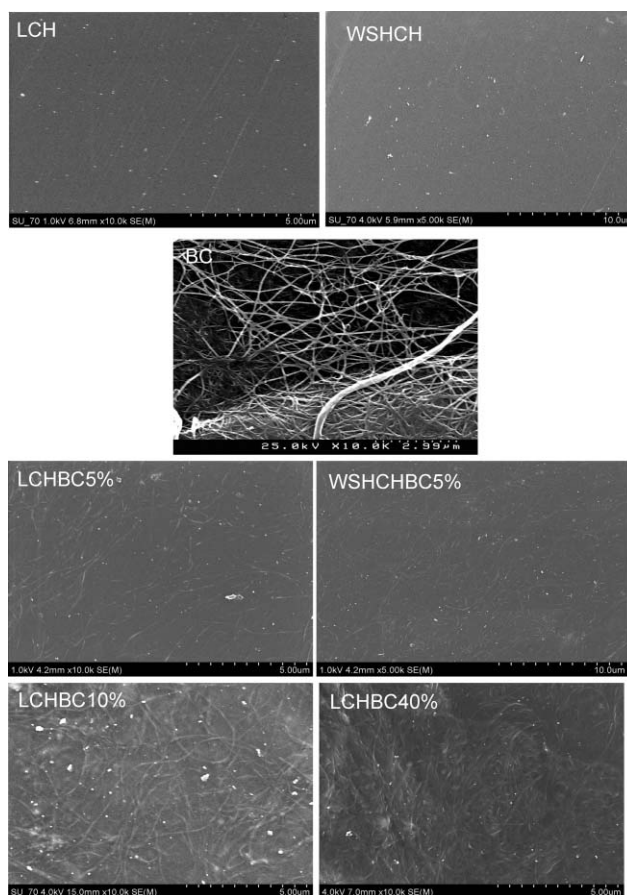

Fig. 2 SEM micrographs of LCH and WSHCH films, BC and the surface of LCH films filled with 5%, 10% 40% of BC and of WSHCH film filled with 5% of BC.

promote the crystallinization of chitosan chains, since the peaks at 2θ 12 and 19° appear in the diffractogram of WSHCHBC films (Fig. 5). This phenomenon is probably explained by the organized deposition of chitosan chains on the surface of the crystalline domains of bacterial cellulose nanofibrils.

Optical properties

The transmittance of the CH and CHBC films (approximately 30 μm thick) is shown in Fig. 6. The transmittance in the range of 400–700 nm was about 90% for HCH and WSHCH chitosan films and about 80% for the LCH film. This difference was probably related to the light-brownish colour of the pristine LCH sample due to the natural occurrence of trace amounts of coloured impurities in some chitosan samples, which however could be removed, if required, using adequate purification procedures.[2] The transmittance values reported here are in good agreement with published transmittance data for chitosan substrates.[36]

In all cases, the transmittance of CH films was not affected by the incorporation of 5% of BC nanofibrils. However, for BC contents equal to or higher than 10%, the transmittance decreased to 80% and 70%, respectively, for HCH/WSHCH and LCH composite films. The high transparency of these new nanocomposites is also evidenced by the pictures showed in Fig. 7.
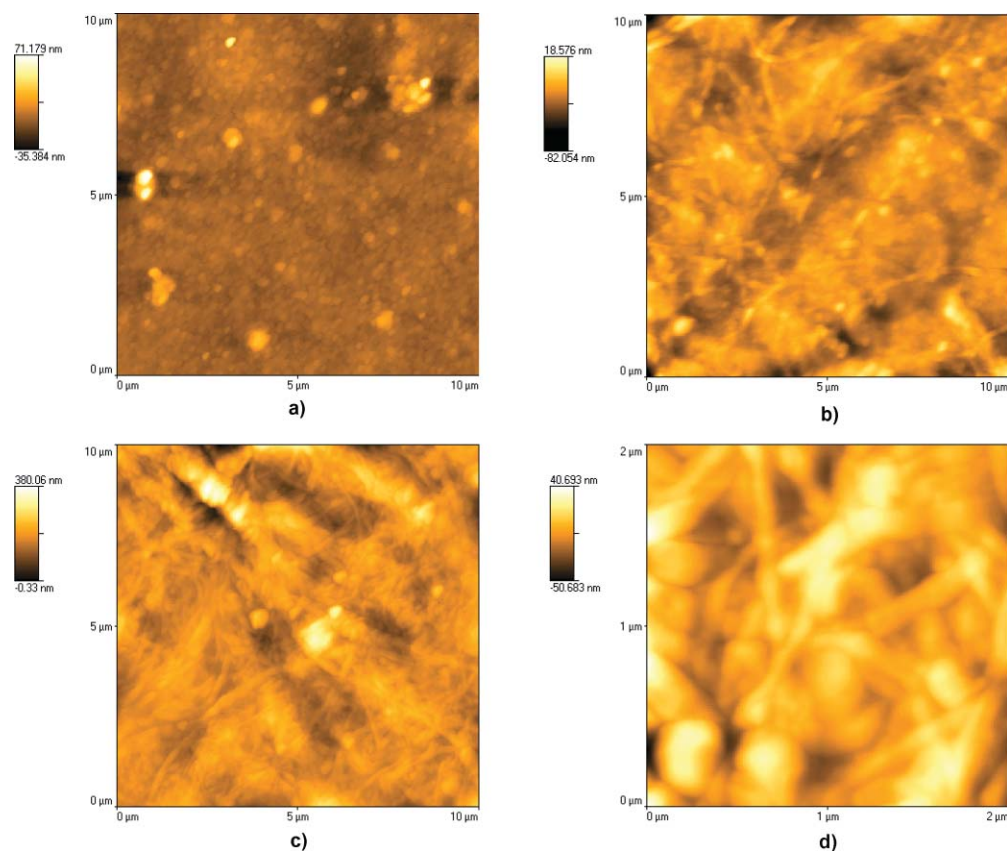
Fig. 3 AFM (tapping mode) topographic images of the surface of a LCH film (a) and of LCHBC nanocomposite films with 10% (b) and 40% (c and d, at two different magnifications) of BC.
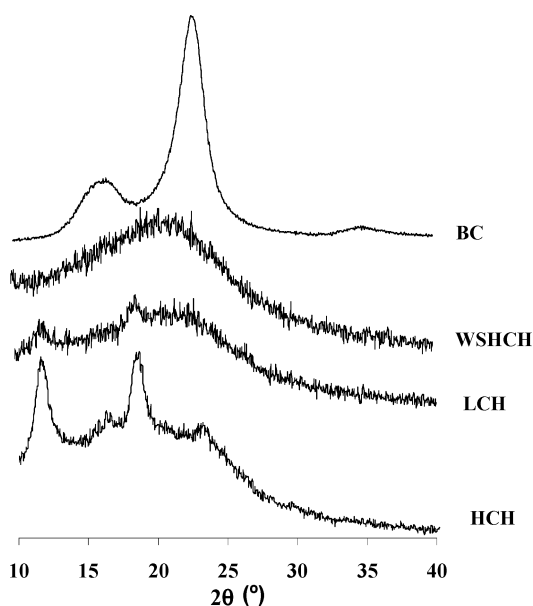
Thermal properties

Thermogravimetric analysis of CH-based films was carried out to evaluate their degradation profiles and thermal stability

Fig. 4 X-Ray diffractograms of BC and CH samples (HCH, LCH and HWSCH).

(Fig. 8, Table 2). In the thermograms of HCH (Fig. 8a) and LCH (not shown), the two mass losses, at around 100 °C and 200 °C, were associated with the volatilization of water and acetic acid, respectively, and the maximum degradation step at 300 °C was assigned to the degradation of chitosan.[37] The WSHCH (Fig. 8a) was more unstable than the unmodified CH, since it started to decompose at around 180 °C with the maximum step at 270 °C. Moreover, in this case the loss of acetic acid was not observed because the films were casted from pure water.

BC showed a typical main double weight-loss feature, with a maximum decomposition temperature in the range of 353–370 °C (Fig. 8a).[38] The mass loss at around 100 °C, associated with the volatilization of water was also observed in this case.

In general, the TGA tracings of the CHBC nanocomposites were a combination of those of CH and BC. The addition of BC to the CH matrices resulted, in most cases, in a slight increase in the thermal stability of the films, as exemplified in Fig. 8b for the WSHCHBC5%. The relevant thermal data (Td_i, Td_1 and Td_2) are shown in Table 2.

Mechanical properties

The effect of the BC content, chitosan DP and quaternization on the large strain behaviour of CHBC composite films was studied up to their failure. The Young modulus, tensile strength and elongation at break, determined from the typical stress-strain curves, are displayed in Fig. 9(a–c).
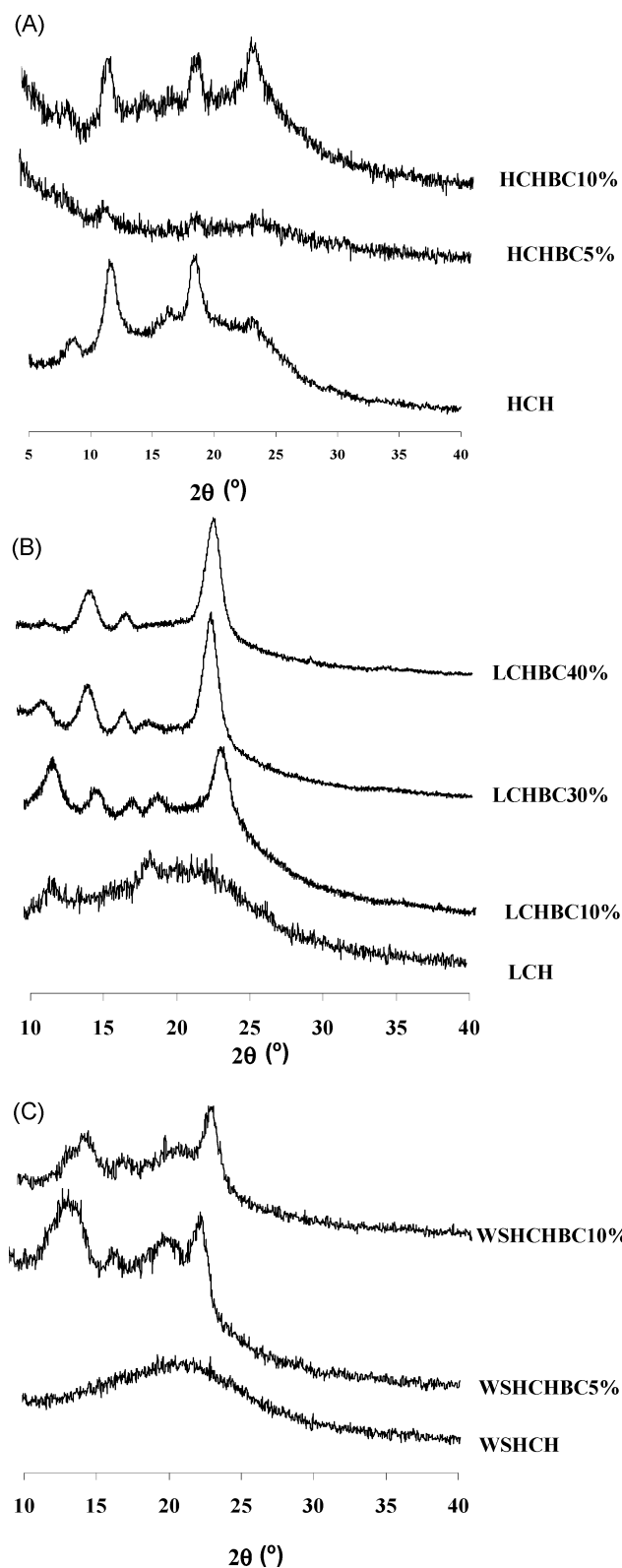
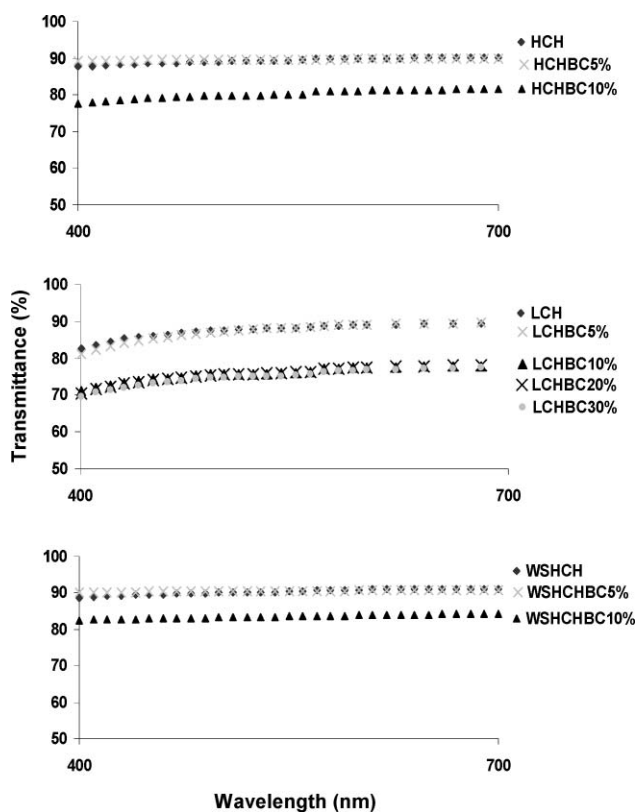**Fig. 5** X-Ray diffractogram of CHBC nanocomposite films.

Fig. 6 Transmittance of unfilled CH films and some corresponding CHBC nanocomposite films with different BC contents.
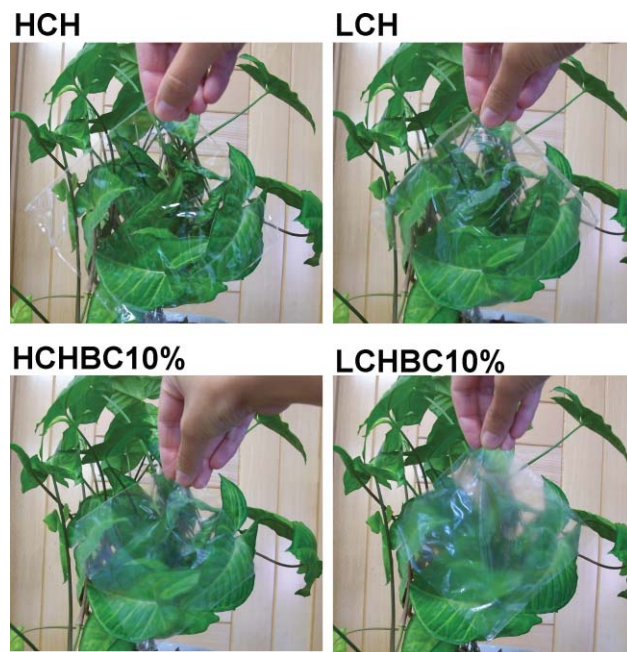

Fig. 7 Images of CH and CHBC nanocomposite films placed in front of a green plant.

behavior of chitosan substrates, associated with the drastic decrease of crystallinity observed by X-ray diffraction.

The Young modulus of the CHBC composite films increased considerably with the BC content (Fig. 9a). At a fiber content of 10%, the Young Modulus was 40, 32 and 114% higher than

As expected, HCH displayed a higher Young modulus than that of LCH.[39] WSHCH displayed the lowest modulus, confirming that this functionalization clearly affected the mechanical

Table 2 Thermal data of the studied samples obtained from the TGA plots

Sample	$T\mathrm{d_i}$ (°C)	$T\mathrm{d_1}$ (°C)	$T\mathrm{d_2}$ (°C)
LCH	237	304 (60)[a]	
LCHBC5%	237	302 (60)	370 (40)
LCHBC10%	237	304 (59)	370 (40)
LCHBC30%	239	300 (66)	379 (56)
LCHBC40%	239	301 (65)	379 (55)
HCH	229	306 (60)	—[b]
HCHBC5%	225	294 (62)	—[b]
HCHBC10%	226	260 (65)	—[b]
WSHCH	186	270 (69)	—[b]
WSHCHBC5%	231	280 (72)	—[b]
WSHCHBC 10%	230	276 (73)	—[b]

[a] Number in parentheses refer to the percentage of residual quantity of materials attained at $T\mathrm{d_1}$ and $T\mathrm{d_2}$. [b] $T\mathrm{d_2}$ is overlapped with $T\mathrm{d_1}$ as shown in Fig. 8b for WSCH derivatives
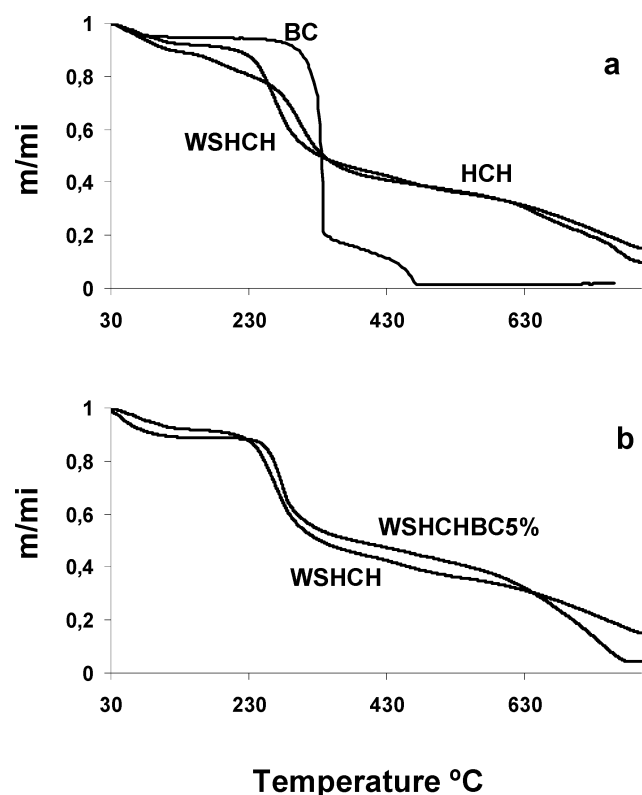
Fig. 8 Thermogravimetric curves for BC, HCH, WSHCH (a) and WSHCHBC5% (b).

Fig. 9 Young modulus, tensile strength and elongation to break of CH samples and corresponding nanocomposite films with different BC contents.

that of the unfilled CH substrates for the HCHBC, LCHBC and WSHCHBC nanocomposite films, respectively. The increment was particularly relevant for the WSHCHBC films, which can be related to the above mentioned increase in crystallinity of this mainly amorphous matrix after incorporation of the BC nanofibrils. Moreover, the LCHBC films with higher BC contents (30 and 40%) presented similar Young moduli to those of HCHBC and WSHCHBC films with only 10% of cellulose nanofibrils. These results indicated that the HCH and the WSHCH matrices are better for the preparation of transparent nanocomposite films with higher mechanical properties.

The incorporation of BC also promoted a considerable increase in the stress of the nanocomposite films (Fig. 9b).
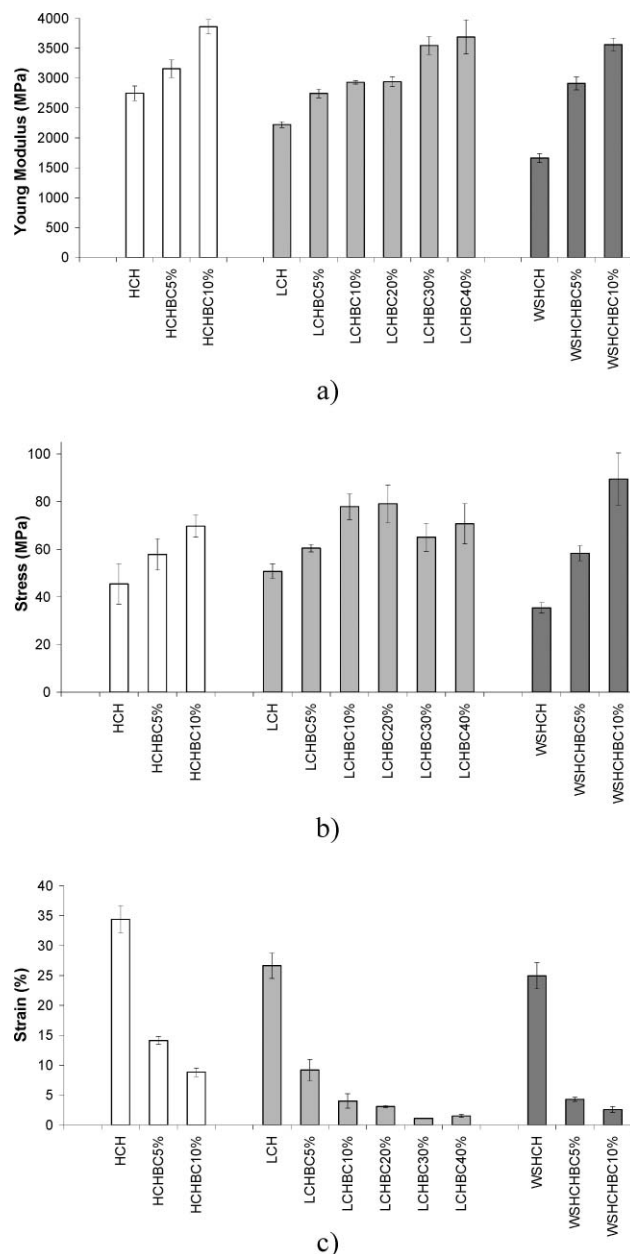
Additionally, the presence of BC caused a significant decrease in the elongation at break (Fig. 9c), which was more pronounced for higher cellulose contents.

The superior mechanical properties of all CHBC films compared with those of the unfilled CH films, confirmed the good interfacial adhesion and the strong interactions between the two components. These results can be explained by the inherent morphology of BC with its nanofibrillar network and the similar structures of the two polysaccharides. In fact, huge increments in the mechanical performance of several composite materials have previously been reported by the incorporation of BC nanofibers (or other nanocellulose substrate) in other kind of matrices, such as phenolic resins.[40]

Conclusion

New chitosan–bacterial cellulose nanocomposite films were prepared by a simple and green procedure based on casting water (or 1% acetic solutions) suspensions of chitosan with different contents of bacterial cellulose. These obtained materials are transparent, flexible and present significantly better mechanical properties than the corresponding unfilled chitosan films. They also have a reasonable thermal stability and low O_2 permeability (preliminary results). Their notable properties are promising for applications in transparent biodegradable and anti-bacterial packaging, medical and electronic devices.

Acknowledgements

References

1 A. Gandini, and M. N. Belgacem, in *Monomers, Polymers and Composites from Renewable Resources*, ed. M. N. Belgacem and A. Gandini, Elsevier, London, 2008, 1–16.

2 C. Peniche, W. Argüelles-Monal, and F. M. Goycoolea, in *Monomers, Polymers and Composites from Renewable Resources*, ed. M. N. Belgacem and A. Gandini, Elsevier, London, 2008, 517–542.

3 V. K. Mourya and N. N. Inamdar, *React. Funct. Polym.*, 2008, **68**, 1013–1051.

4 M. Mucha and A. Pawlak, *Thermochim. Acta*, 2005, **427**, 69–76.

5 A. Pawlak, and A. Mucha, in *29th Conference of the North American Thermal Analysis Society*, Elsevier Science Bv, St Louis, Michigan, 2001, 153–166.

6 K. Sakurai, T. Maegawa and T. Takahashi, *Polymer*, 2000, **41**, 7051–7056.

7 M. M. Amiji, *Biomaterials*, 1995, **16**, 593–599.

8 A. Sionkowska, M. Wisniewski, J. Skopinska, C. J. Kennedy and T. J. Wess, *J. Photochem. Photobiol., A*, 2004, **162**, 545–554.

9 L. Fang and S. H. Goh, *J. Appl. Polym. Sci.*, 2000, **76**, 1785–1790.

10 Y. K. Twu, H. I. Huang, S. Y. Chang and S. L. Wang, *Carbohydr. Polym.*, 2003, **54**, 425–430.

11 Y. B. Wu, S. H. Yu, F. L. Mi, C. W. Wu, S. S. Shyu, C. K. Peng and A. C. Chao, *Carbohydr. Polym.*, 2004, **57**, 435–440.

12 S. Z. Rogovina and G. A. Vikhoreva, *Glycoconjugate J.*, 2006, **23**, 611–618.

13 M. Hasegawa, A. Isogai, F. Onabe, M. Usuda and R. H. Atalla, *J. Appl. Polym. Sci.*, 1992, **45**, 1873–1879.

14 S. Z. Rogovina, T. A. Akopova, G. A. Vikhoreva, S. N. Zelenetskii, I. N. Gorbacheva and N. V. Suslova, *Polym. Sci. Ser. B*, 2001, **43**, 265–268.

15 J. M. Urreaga and M. U. de la Orden, *Eur. Polym. J.*, 2006, **42**, 2606–2616.

16 D. Nordqvist, J. Idermark and M. S. Hedenqvist, *Biomacromolecules*, 2007, **8**, 2398–2403.

17 Y. Kim, R. Jung, H. S. Kim and H. J. Jin, *Curr. Appl. Phys.*, 2009, **9**, S69–S71.

18 H. Fukuzumi, T. Saito, T. Wata, Y. Kumamoto and A. Isogai, *Biomacromolecules*, 2009, **10**, 162–165.

19 R. Jung, H. S. Kim, Y. Kim, S. M. Kwon, H. S. Lee and H. J. In, *J. Polym. Sci., Part B: Polym. Phys.*, 2008, **46**, 1235–1242.

20 Y. Shimazaki, Y. Miyazaki, Y. Takezawa, M. Nogi, K. Abe, S. Ifuku and H. Yano, *Biomacromolecules*, 2007, **8**, 2976–2978.

21 M. Nogi, S. Iwamoto, A. N. Nakagaito and H. Yano, *Adv. Mater.*, 2009, **21**, 1595–1598.

22 S. Ifuku, M. Nogi, K. Abe, K. Handa, F. Nakatsubo and H. Yano, *Biomacromolecules*, 2007, **8**, 1973–1978.

23 M. Nogi, K. Handa, A. N. Nakagaito and H. Yano, *Appl. Phys. Lett.*, 2005, **87**, 243110.

24 M. Nogi, S. Ifuku, K. Abe, K. Handa, A. N. Nakagaito and H. Yano, *Appl. Phys. Lett.*, 2006, **88**, 133124.

25 M. Nogi and H. Yano, *Adv. Mater.*, 2008, **20**, 1849–1852.

26 D. Ciechanska, *Fibres Text. East. Eur.*, 2004, **12**, 69–72.

27 M. Phisalaphong and N. Jatupaiboon, *Carbohydr. Polym.*, 2008, **74**, 482–488.

28 V. Dubey, L. K. Pandey and C. Saxena, *J. Membr. Sci.*, 2005, **251**, 131–136.

29 H. S. Seong, H. S. Whang and S. W. Ko, *J. Appl. Polym. Sci.*, 2000, **76**, 2009–2015.

30 M. Rinaudo, M. Milas and L. P. Dung, *Int. J. Biol. Macromol.*, 1993, **15**, 281–285.

31 J. Desbriéres, C. Martinez and M. Rinaudo, *Int. J. Biol. Macromol.*, 1996, **19**, 21–28.

32 Z. Zheng, L. Zhang, L. Kong, A. Wang, Y. Gong and X. Zhang, *J. Biomed. Mater. Res., Part A*, 2009, **89a**, 453–465.

33 R. J. Samuels, *J. Polym. Sci., Part B: Polym. Phys.*, 1981, **19**, 1081–1105.

34 G. Ma, D. Yang, Y. Zhou, M. Xiao, J. F. Kennedy and J. Nie, *Carbohydr. Polym.*, 2008, **74**, 121–126.

35 D. N.-S. Hon, *Chemical Modification of Lignocellulosic Materials*, Marcell Dekker, New York, 1996.

36 A. Larena and D. A. Caceres, *Appl. Surf. Sci.*, 2004, **238**, 273–277.

37 M. J. Zohuriaan and F. Shokrolahi, *Polym. Test.*, 2004, **23**, 575–579.

38 D. Klemm, B. Philipp, T. Heinze, U. Heinze, and W. Wagenknecht, *Comprehensive Cellulose Chemistry*, vol. 1, Wiley-VCH, Weinheim, 1998.

39 R. H. Chen and H. D. Hwa, *Carbohydr. Polym.*, 1996, **29**, 353–358.

40 A. N. Nakagaito, S. Iwamoto and H. Yano, *Appl. Phys. A: Mater. Sci. Process.*, 2005, **80**, 93–97.